Biochimica et Biophysica Acta 1838 (2014) 2607–2614

Contents lists available at ScienceDirect

Biochimica et Biophysica Acta

journal homepage: www.elsevier.com/locate/bbamem

Ionomycin causes susceptibility to phospholipase A_2 while temperature-induced increases in membrane fluidity fail: Possible involvement of actin fragmentation

Elizabeth Gibbons, Michael Murri, Amy Grabner, Eric Moss, Lauryl Campbell, Jennifer Nelson, Allan M. Judd, John D. Bell *

Department of Physiology and Developmental Biology, Brigham Young University, Provo, UT 84602, USA

ARTICLE INFO

Article history:
Received 30 January 2014
Received in revised form 10 May 2014
Accepted 30 May 2014
Available online 3 July 2014

Keywords:
TMA-DPH
Patman
Merocyanine 540
Membrane order
Phalloidin
Cytoskeleton

ABSTRACT

A diminution in the order of membrane lipids, which occurs during apoptosis, has been shown to correlate with increased membrane susceptibility to hydrolysis by secretory phospholipase A_2. Studies with artificial membranes, however, have demonstrated that the relationship between membrane order and hydrolysis is more complex than suggested thus far by cell studies. To better resolve this relationship, this study focused on comparisons between increasing temperature and calcium ionophore as means of decreasing membrane order in S49 cells. Although these two treatments caused comparable changes in apparent membrane order as detected by steady-state fluorescence measurements, only ionophore treatment enhanced phospholipase activity. Experiments with exogenously-added phosphatidylserine indicated that the difference was not due to the presence of that anionic phospholipid in the outer membrane leaflet. Instead, analysis of the equilibration kinetics of various cationic membrane probes revealed that the difference could relate to the spacing of membrane lipids. Specifically, ionophore treatment increased that spacing while temperature only affected overall membrane order and fluidity. To consider the possibility that the distinction with ionophore might relate to the actin cytoskeleton, cells were stained with phalloidin and imaged via confocal microscopy. Ionophore caused disruption of actin fibers while increased temperature did not. This apparent connection between membrane hydrolysis and the cytoskeleton was further corroborated by examining the relationship among these events during apoptosis stimulated by thapsigargin.

1. Introduction

Prior studies have investigated the role of biophysical alterations to the plasma membrane that govern its susceptibility to hydrolysis by secretory phospholipase A_2 ($sPLA_2$). Environment-sensitive fluorescent membrane probes such as merocyanine 540, Laurdan, diphenylhexatriene derivatives, and Patman have been used to detect changes in lipid order that correlate temporally and quantitatively with susceptibility [1–6]. In lymphocytes, reductions in lipid order consistently correlate with conditions that render the cells vulnerable to $sPLA_2$[1,2,6,7]. This apparent reduction in lipid order has been detected only by probes sensitive to the head-group region of the membrane and have been quantified from steady-state measurements of generalized polarization (GP) of the naphthalene derivatives (Laurdan and Patman) or probe anisotropy [1,2,6,7]. However, experiments with artificial bilayers and human erythrocytes have demonstrated that the relationship between membrane order and $sPLA_2$ activity is more complex than implied by the results from nucleated cells. For example, under some conditions, raising the experimental temperature reduces the order of liposome membranes and yields the same changes in probe steady-state fluorescence observed in cells, yet the rate of hydrolysis by $sPLA_2$ is not affected [8–10]. In erythrocytes, conditions that promote hydrolysis actually increase the average lipid order, but in a way that enhances the structural diversity in the membrane. Hydrolysis by $sPLA_2$ appears to localize at boundaries along regions of that diversity [3,4,11].

Hence, if membrane lipid order is relevant to the activity of $sPLA_2$, there must be additional information about those properties that cannot be discerned from the anisotropy or GP of these probes. Recent studies suggested that monitoring the pre-steady-state equilibration of Patman may provide that additional information. Patman is an analog of Laurdan that contains a trimethylammonium group attached to the naphthalene moiety to minimize transbilayer migration and a two-carbon extension of the aliphatic tail to retain the probe in the membrane [12]. Specifically, analysis of Patman kinetics distinguished subtle

* Corresponding author. Tel.: +1 801 422 2353.
E-mail addresses: liz.gibbons7@gmail.com (E. Gibbons), cougarmurri@gmail.com (M. Murri), amynicole7@gmail.com (A. Grabner), ericfmoss@gmail.com (E. Moss), laurylcampbell@gmail.com (L. Campbell), jennelson5@gmail.com (J. Nelson), allan_judd@byu.edu (A.M. Judd), john_bell@byu.edu (J.D. Bell).

http://dx.doi.org/10.1016/j.bbamem.2014.05.028
0005-2736/

differences between reductions in bilayer order in cells when $sPLA_2$ activity is enhanced [6] compared to those in artificial membranes that do not affect hydrolysis [9]. The results of this comparison supported the hypothesis that $sPLA_2$ activity is promoted by changes in membrane order only when those changes facilitate migration of phospholipid molecules perpendicular to the plane of the bilayer [6,13,14]. Consequently, it was proposed that quantifying the kinetics of Patman equilibration in addition to measuring its end-point GP can be an effective tool for detecting these subtleties of membrane order.

This study was designed to test this hypothesis and proposal in cells without relying on artificial bilayers. This was accomplished by comparing two experimental conditions that produce the same changes in membrane properties detected by the end-point fluorescence of environment-sensitive membrane probes yet differ in their ability to stimulate hydrolysis by $sPLA_2$. A known paradigm for producing changes in membrane properties that induce hydrolysis by $sPLA_2$ is cellular apoptosis [1,2,6,15]. In this study, the calcium ionophore ionomycin was chosen to induce cell death because its effects are rapid, uniform, and synchronous [1]. In order to produce changes in steady-state probe fluorescence without stimulating $sPLA_2$ activity, sample temperature was manipulated. Comparison of these two treatments was then used to clarify the nature of the relationship between membrane physical properties and $sPLA_2$ activity in cells.

2. Materials and methods

2.1. Reagents

Monomeric aspartate-49 $sPLA_2$ from the venom of *Agkistrodon piscivorus piscivorus* (AppD49) was isolated and prepared as described [16]. Ionomycin, 1-(4-trimethylammoniumphenyl)-6-phenyl-1,3,5-hexatriene (TMA-DPH), acrylodan-labeled fatty acid-binding protein (ADIFAB), 6-palmitoyl-2-[[2-(trimethylammonio) ethyl]-methylamino]naphthalene chloride (Patman), merocyanine 540 (MC540), and phalloidin and annexin V conjugates with Alexa Fluor® 488 were purchased from Life Technologies (Grand Island, NY). Thapsigargin (TG) was acquired from Life Technologies or Enzo Life Sciences (Plymouth Meeting, PA). Formaldehyde (16%, no methanol) was obtained from Thermo Fisher Scientific (Rockford, IL). Porcine brain L-α-phosphatidylserine (PS) and chicken egg L-α-phosphatidylcholine (PC) were purchased from Avanti Polar Lipids (Birmingham, AL). All other reagents were obtained from standard suppliers.

2.2. Cell culture and treatment with agents

S49 mouse lymphoma cells were grown in suspension in Dulbecco's Modified Eagle Medium at 37 °C (10% CO_2) as explained [17]. Thapsigargin treatments (5 μM) or equivalent volumes of DMSO (0.1% v/v) were done in culture medium. For experiments, cells were collected by centrifugation, washed, and suspended ($0.25–3.5 \times 10^6$ cells/ml) in a balanced salt medium (NaCl = 134 mM, KCl = 6.2 mM, $CaCl_2$ = 1.6 mM, $MgCl_2$ = 1.2 mM, Hepes = 18.0 mM, and glucose = 13.6 mM, pH 7.4, 37 °C). Treatments with ionomycin (300 nM) were done in the balanced salt medium after cell harvesting. All experiments, treatments, and incubations were conducted at 37 °C unless otherwise specified. Samples were equilibrated at the indicated temperature for at least 10 min prior to addition of probes or treatment agents. Sample viability was assessed by trypan blue exclusion.

2.3. Addition of exogenous PS

S49 cell plasma membranes were enriched with exogenous PS using liposomes containing 50% PS and 50% PC. Lipids were dried under nitrogen and resuspended in PBS (1 mM final). In order to make unilamellar liposomes, samples were sonicated in a Misonex Sonicator 3000 (Farmingdale, NY) at 2 W for 3 min. Cells were harvested as described above and resuspended to a density of $0.5–1.5 \times 10^6$ cells/ml. Cells were then incubated with liposomes (50 μM final lipid concentration) for 30 min at 37 °C, collected by centrifugation, and resuspended in balanced salt medium for experimentation.

2.4. Fluorescence spectroscopy

Time-based fluorescence intensities were assayed with a Fluoromax (Horiba Jobin Yvon, Edison, NJ) photon-counting spectrofluorometer. Anisotropy measurements were collected with a PC-1 (ISS, Champaign, IL) photon-counting spectrofluorometer equipped with Glan–Thompson polarizers. Continuous gentle stirring with a magnetic stir bar ensured sample homogeneity, and temperature was maintained by a jacketed sample chamber fed by a circulating water bath. Bandpass was set at 16 nm for anisotropy measurements and 4 nm for all other experiments. When necessary, fluorescence emission at multiple wavelengths was acquired by rapid sluing of monochromator mirrors. Cell samples were treated and prepared as described above and equilibrated in the fluorometer sample chamber for at least 5 min before initiating data acquisition.

Cell membrane hydrolysis catalyzed by $sPLA_2$ was measured by assaying fatty acid release using ADIFAB (65 nM final) as described [18]. The amount of fatty acid released was quantified by comparing ADIFAB fluorescence emission (excitation = 390 nm) at 432 and 505 nm (I_{432} and I_{505}) [19] and calculating the generalized polarization (GP_{ADIFAB}) as described [17]:

$$GP_{ADIFAB} = \frac{I_{505} - I_{432}}{I_{505} + I_{432}}. \quad (1)$$

Measurements of TMA-DPH (250 nM final) fluorescence were collected with different configurations of excitation (350 nm) and emission (452 nm) polarizers in the vertical and horizontal positions after 10 min equilibration of cells with the probe. The anisotropy (r) was then calculated from the fluorescence intensity when both polarizers were vertical ($I_{//}$) and when the excitation was vertical and the emission horizontal ($I_{\perp}$). Correction for differential transmission and detection at the two polarizer positions was included (G) according to convention:

$$r = \frac{I_{//} - GI_{\perp}}{I_{//} + 2GI_{\perp}}. \quad (2)$$

Merocyanine 540 (170 nM) fluorescence intensity was acquired as a function of time with excitation at 540 nm and emission at 585 nm. Patman (250 nM final) data were collected in a similar manner with excitation at 350 nm and emission at both 435 and 500 nm (I_{435} and I_{500}). Patman spectral changes were quantified by calculating the generalized polarization (GP) as follows [20]:

$$GP = \frac{I_{435} - I_{500}}{I_{435} + I_{500}}. \quad (3)$$

For Patman equilibration analyses of temperature studies, time courses of probe intensity were smoothed by nonlinear regression to an arbitrary function (analogous to Eq. (4)) and normalized to the intensity at 435 nm at 400 s to aggregate data from multiple replicate samples. These pooled data were then fit by nonlinear regression to the following:

$$I = A\left(1 - e^{-bt}\right) + C\left(1 - e^{-dt}\right) + F \quad (4)$$

where A and C are arbitrary scalars, b and d are rate constants, and F is the intercept intensity. Intensities at both wavelengths were fit together with b and d constrained as shared parameters. These fitting parameters were then used to calculate model parameter values (fraction of probe

in each configuration, environmental polarity of each configuration, and rate of probe entering each configuration) according to Eqs. (11)–(14) in Franchino et al. [9]. Error was evaluated by using the extreme values of the 95% confidence intervals for each fitting parameter generated by nonlinear regression. Every permutation of these fitting parameters was inputted into Franchino et al. Eqs. (11)–(14) [9] to determine the range of possible model parameter values.

For Patman equilibration studies with ionomycin, the ionophore was added after probe. These intensity profiles were fit according to an arbitrary function similar to Eq. (4) for both 435 and 500 nm with a third exponential term (i.e. analogous to the first term, $A(1-e^{-bt})$, in Eq. (4)) applied at the time of ionomycin addition. The rate constant of this third exponential term was constrained to be shared between the 435 nm and 500 nm curves. Intensity changes were assessed by the value of the scaler from this third term.

2.5. Flow cytometry

The annexin V Alexa Fluor® 488 conjugate was used to assay PS externalization according to manufacturer's instructions. All flow cytometry samples were immediately processed (without fixation) in a BD FACSCanto flow cytometer (BD Biosciences, San Jose, CA) with an argon excitation laser (488 nm). Emission was assessed using a bandpass filter at 515–545 nm. Resulting histograms of annexin V fluorescence intensity were fit by nonlinear regression with a function composed of three Gaussian curves (low, medium, and high annexin V intensities). In cases of samples labeled with exogenous PS, four Gaussian curves were required to fit the data, and the two with the highest means were assigned to the "high" category. The means were constrained to be shared among the various samples for each experiment.

2.6. Phalloidin confocal microscopy

Cells were simultaneously fixed, permeabilized, and stained with fluorescent phalloidin (Alexa Fluor® 488) according to the manufacturer's protocol. After being mounted onto slides, cells were stained with a solution containing 165 nM phalloidin, 3.7% formaldehyde, 1% bovine serum albumin, and 0.1 mg/ml 1-palmitoyl-2-hydroxy-sn-glycero-3-phosphocholine for 20 min at 4 °C. Slides were then washed with buffer before coverslips were mounted. Images were collected on an Olympus (Center Valley, PA) FluoView FV 300 confocal laser scanning microscope using a 60× oil immersion objective lens and 488 nm argon excitation laser.

ImageJ software was used to quantify the circularity index and size (number of pixels) of all particles in each image [21]. Prior to analysis, color images were converted to 8-bit grayscale and inverted so that particles were dark against a light background. The default algorithm in the software package for determining background levels was used. After subtracting this background, images were converted to 1-bit black and white.

3. Results and discussion

3.1. Comparison of effects of temperature and ionomycin on membrane order and hydrolysis

Experiments with the fluorescent probes TMA-DPH and Patman were conducted to assess whether cell membrane biophysical properties could be manipulated by temperature to an extent comparable to that observed during ionophore treatment. As shown in Fig. 1A, TMA-DPH anisotropy decreased as temperature was elevated (gray bars), consistent with the membrane becoming more disordered as temperature was raised. Subsequent addition of ionomycin caused a further drop in anisotropy at all temperatures (black bars), suggesting that the two effects on membrane order could involve different mechanisms. A two-way analysis of variance indicated that ionophore treatment was

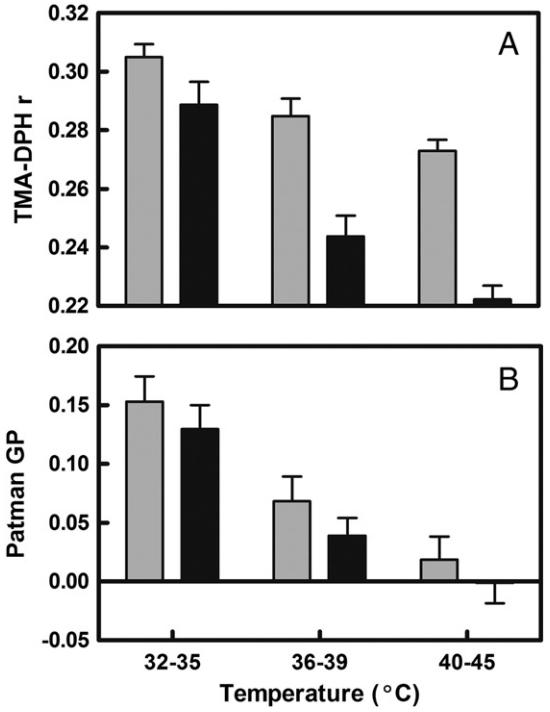

Fig. 1. Effect of temperature and ionomycin on TMA-DPH anisotropy and Patman GP. Cells were equilibrated at the indicated temperatures for 10 min with TMA-DPH (Panel A) or Patman (Panel B), and data were then acquired as described in Materials and methods. Ionomycin was then added and additional data were acquired. The gray bars represent the value of anisotropy (A) or GP (B) acquired immediately before ionomycin addition. The black bars represent the effect of ionomycin treatment assessed at 2 min (A) or at the GP minimum (B, generally achieved within 2 min after adding ionomycin). Error bars represent the SE (n = 9–12 per group).

responsible for 31.9% of the variation within the data ($p < 0.0001$), temperature accounted for 24.4% of the variation ($p < 0.0001$), and no significant interaction between the two was detected (4% of total variation; $p = 0.09$, n = 9–12 per group). Importantly, the effect of temperature was comparable to the effect of addition of ionomycin (average change in anisotropy induced by ionomycin = −0.034 units; average change by heating from 32 to 45 °C = −0.048 units, a ratio of 0.72).

When Patman was used to assess membrane order (Fig. 1B), there was also a significant negative trend in Patman GP over the same temperature range (gray bars), and ionomycin treatment caused a further reduction in GP at all temperatures (black bars). Two-way analysis of variance showed that both temperature and ionomycin effects were significant without interaction (temperature: $p = 0.0001$, 42% of the variation; ionomycin: $p < 0.0001$, 2% of the variation; interaction: $p = 0.6$, 0.05% of variation; n = 9–15 per group). An interesting difference from the TMA-DPH result is that in the case of Patman, the effect of ionomycin was much smaller than the effect of heating from 32 to 45 °C (average change in GP induced by ionomycin = −0.024 units; average change by heating from 32 to 45 °C = −0.15 units, a ratio of 0.17). This difference between the observations with TMA-DPH and Patman further reinforced the possibility that the effects of temperature and ionomycin on apparent membrane order were not the same.

In summary, the results of Fig. 1 demonstrate that elevation of temperature from 32 to 45 °C is sufficient to produce a change in apparent membrane order comparable to (Panel A) or greater than (Panel B) that generated by ionomycin treatment. For that reason, untreated cells at 32 °C was used as the reference point to determine whether the membrane changes associated with temperature elevation could enhance $sPLA_2$-catalyzed hydrolysis by the same increment as ionomycin treatment. Accordingly, hydrolysis at this reference point was compared to that observed with untreated cells at 45 °C or ionomycin-treated cells at

32 °C. Previous experiments demonstrated that the temperature dependence of AppD49 $sPLA_2$ activity toward micelles is minimal in this temperature range compared to the magnitude of effects of membrane structure [3]. Fig. 2 shows example profiles of $sPLA_2$-catalyzed hydrolysis (assayed by ADIFAB GP) over time, with an increase in GP indicating fatty acid release from the plasma membrane. As shown by the upper (black) curve, the presence of ionomycin produced a large increase in ADIFAB GP when $sPLA_2$ was added (dotted line) compared to that observed in the reference sample (middle dark gray curve). This result suggested that the ionophore rendered the cells susceptible to attack by $sPLA_2$ similar to previous observations reported for 37 °C [1]. The question, then, was whether cells at 45 °C would behave more like the 32 °C reference or the ionomycin-treated sample. The lower (light gray) curve illustrates that incubating the sample at 45 °C produced a hydrolysis profile indistinguishable from the reference obtained at 32 °C. This result was reproducible ($p = 0.1$ comparing 8 samples at 45 °C to the 32 °C reference and $p < 0.0001$ comparing them to the ionomycin-treated sample at 32 °C, t-tests). Adding ionomycin to samples at 45 °C resulted in complete cell susceptibility to hydrolysis by $sPLA_2$ identical to the observation at 32 °C (not shown). Therefore, although raising the temperature caused the same or greater changes in TMA-DPH and Patman fluorescence as ionomycin, only the ionophore produced a significant increase in susceptibility to $sPLA_2$.

3.2. Direct effects of phosphatidylserine

A possible candidate for the distinction between ionomycin treatment and temperature elevation was PS exposed on the outer surface of the plasma membrane. It is well known that ionomycin causes a large enhancement of PS externalization [22–24] and that such exposure could enhance $sPLA_2$ activity [7,18,24]. To verify the distinction between ionomycin and temperature effects on PS exposure, measurements of the amount of PS present on the cell surface were made using fluorescent annexin V. Flow cytometry data validated that temperature elevation from 32 to 45 °C does not alter the level of PS on the cell surface ($p = 0.3$ by analysis of variance, n = 4 each at 32, 37, and 45 °C; distinguishable from ionomycin-treated positive control, $p < 0.001$). To test the hypothesis that PS is the source of differences in hydrolysis observed in Fig. 2, exogenous PS was added directly to the outer leaflet of the plasma membrane. This was accomplished by incubating cells with vesicles composed of 50% egg PC and 50% brain PS. Successful delivery was assessed by flow cytometry. Fig. 3 shows histograms of external PS exposure for control cells (gray) and cells incubated with vesicles containing PS (black). The enhancement of

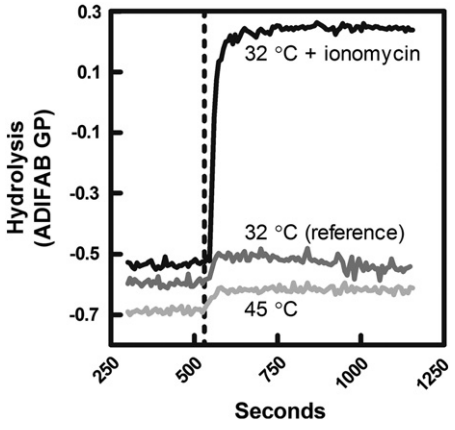

Fig. 2. Cell membrane hydrolysis by $sPLA_2$ at 32 and 45 °C. Cells were incubated at 32 (dark gray and black) or 45 °C (light gray) for 5 min and ionomycin (black) or control solvent (DMSO; dark and light gray) for an additional 5 min prior to data acquisition. Hydrolysis was assayed using ADIFAB (added at t = 0 on graph) as described in Materials and methods. Secretory PLA_2 was added at the dotted line. Data were numerically displaced vertically for clarity of presentation.

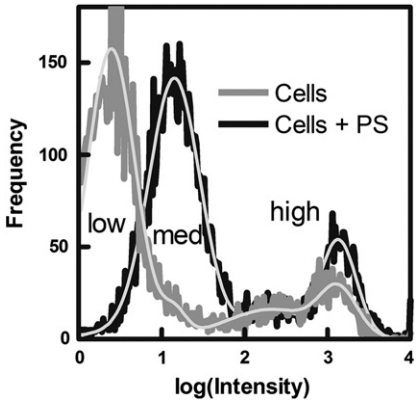

Fig. 3. Addition of exogenous PS to plasma membrane. Cells were incubated with (black) or without (gray) PS-containing liposomes and assayed for annexin V binding as described in Materials and methods. Example flow cytometry histograms show the designation of low, medium ("med"), and high annexin V intensities.

annexin staining at both medium and high intensities shown in Fig. 3 was reproducible ($p = 0.02$ for each, t test). Control experiments verified that addition of exogenous PS did not alter membrane order as detected by TMA-DPH anisotropy nor the ability of ionomycin to subsequently reduce it (i.e. as in Fig. 1; vesicles contributed 6% of the variation, $p = 0.4$; ionomycin contributed 28% of the variation, $p = 0.001$; interaction contributed 0.4% of the variation, $p = 0.6$; two-way analysis of variance, n = 5 per group).

After incubation of cells with these vesicles, samples were assayed for susceptibility to $sPLA_2$ by repeating the experiments of Fig. 2. Two-way analysis of variance indicated that there were no significant effects of either temperature or the presence of exogenously-added PS on the amount of hydrolysis observed upon addition of $sPLA_2$ ($p = 0.9$ for temperature, 0.3 for PS, and 0.8 for interaction, in combination accounted for only 3% of the variation, n = 5–14 per group). It could be argued that hydrolytic susceptibility was not affected because the bulk of the annexin V positive cells in Fig. 3 was stained with lower intensity than seen in ionomycin-treated samples (largely staining at the "high" intensity) [7]. To investigate this possibility, parallel annexin V and susceptibility assays were compared to determine if the percentage of cells with "high" intensity staining correlated with the amount of fatty acid release from the membrane. Linear regression revealed that there was no significant correlation between ADIFAB GP increase (hydrolysis) and cells with "high" intensity annexin V staining in control cells or cells loaded with exogenous PS ($p = 0.4$, $r^2 = 0.2$ and 0.3, $r^2 = 0.3$ respectively, n = 5 per group).

3.3. Differences detected by Patman, TMA-DPH, and MC540 fluorescence intensity

Since the presence of PS on the outer leaflet of the cell membrane did not appear to be the distinction between ionomycin treatment and temperature elevation, attention was directed toward a more detailed analysis of the biophysical properties of the bilayer. First, the possibility that the distinction was due to ultrastructural changes such as cell shrinkage and microparticle shedding from the plasma membrane was considered. These effects are known to occur in S49 cells and result from osmotic effects due to opening of calcium-activated potassium channels during ionophore treatment [11,25–27]. To test this possibility, the experiments of Figs. 2 and 3 were repeated in the presence of 1 mM quinine, an inhibitor of calcium-activated potassium flux. Quinine had no effect on the ability of ionomycin to induce susceptibility even though it has been shown to reduce the release of microparticles by 80% in S49 cells [27]. This result is consistent with similar findings from studies with erythrocytes [11].

Second, attention was turned to molecular-scale changes in the membrane. Previous studies with Patman revealed that examining the time course of probe equilibration can detect biophysical membrane changes that are otherwise indistinguishable by endpoint measurements of anisotropy or GP [6,9]. In those studies, a minimum model that could account for the equilibration patterns was identified. This model required two membrane-bound configurations for Patman that differ in their rates of equilibration. Molecular dynamics simulations using a related probe, Laurdan, also predicted that these probes might exist in two equilibrium configurations and identified possible molecular bases for the two [28]. From the kinetics of Patman equilibration at two wavelengths (435 and 500 nm), the model generates the proportion of Patman in each configuration, the relative environmental polarity of each, and the equilibration rate of each. Accordingly, Patman emission intensities at both wavelengths were collected over time for at least 500 s after the probe was added to cell samples at various temperatures between 32 and 45 °C. The data were fit by nonlinear regression with an arbitrary function analogous to Eq. (4) and analyzed according to the model [6,9]. Similar to results reported previously for the effect of temperature on artificial membranes [9], the only model parameter consistently altered by temperature was the environmental polarity of one of the configurations. This polarity increased from 0.336 ± 0.052 to 0.443 ± 0.002 arbitrary units (mean ± 95% confidence interval) from low to high temperature. Overlap of the confidence intervals for all other model parameters indicated that they were not affected by temperature.

In order to determine whether calcium ionophore treatment had the same effect on the membrane as temperature, an experimental protocol was adopted in which ionomycin was added midway during Patman's equilibration (Fig. 4A). This procedure was used to leverage the precision of before- and after-treatment measurements on the same sample since the effects of ionomycin on Patman fluorescence were subtle (i.e. the change in GP was small, compared to effects of temperature, Fig. 1B). Surprisingly, addition of ionomycin caused an increase in the intensity at both wavelengths. This result was reproducible (Fig. 4B) and sharply contrasted the more conventional result observed with temperature (in which total intensity remains constant and differences in membrane order are reflected by symmetrical but opposite changes at 435 and 500 nm). Since Patman fluorescence in aqueous solution is negligible [9], these results suggest that ionomycin treatment increases the capacity of the membrane to bind the probe. Importantly, these changes in Patman emission occurred within a few minutes (rate = $0.011 \pm 0.003\ s^{-1}$, half-time of 61 s) a time frame during which biological effects of ionomycin on S49 cells are known to occur [1,27], but preceding latent effects on membrane permeability that would obscure interpretations of membrane probe fluorescence (generally beyond 10 min based on control imaging experiments and [6]).

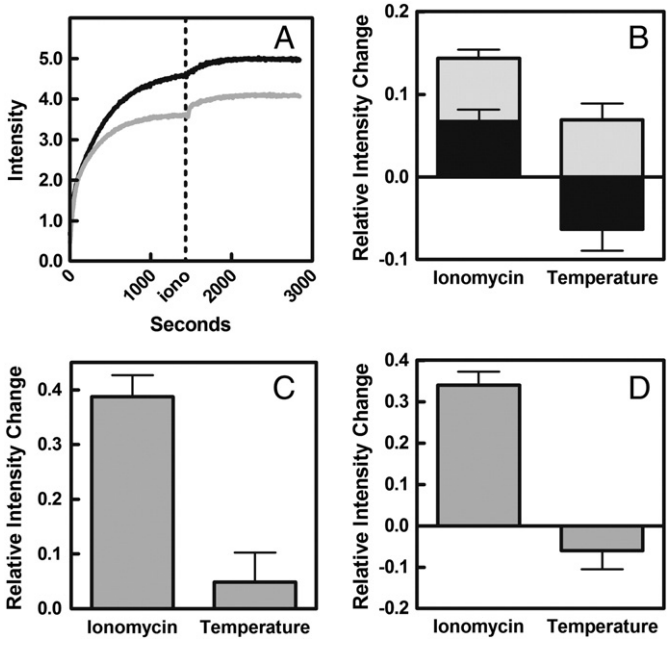

Fig. 4. Membrane probe intensity changes after ionomycin treatment or temperature elevation. Panel A: Patman emission intensity was assayed at 435 (black) and 500 nm (gray) following Patman addition to the cell sample (time 0 on the graph) 38 °C. Ionomycin was added at the dotted line. Panel B: Patman emission intensity was quantified from profiles such as that shown in Panel A at both 435 (black) and 500 nm (gray), before and after ionomycin treatment, and at temperatures ranging from 32 to 45 °C. Bars represent the average change in these intensities after ionomycin treatment or the difference between average sample intensity at high (40–45 °C) and low temperatures (32–35 °C). Panels C and D: Merocyanine 540 (C) and TMA-DPH (D) intensities were assayed at temperatures ranging from 32 to 45 °C as described in Materials and methods. The bars represent the average change in these intensities following 2 min of treatment with ionomycin or the difference between the average intensities at high (40–45 °C) and low temperatures (32–35 °C). Error bars represent the SE (n = 9–34 per group).

To test the generality of this observation, we compared two other charged membrane probes with modest water solubility for which binding should depend on membrane biophysics (MC540 [10,29–31] and TMA-DPH). As shown in Fig. 4C and D, temperature did not influence the total fluorescence intensity of either TMA-DPH or MC540, indicating that temperature probably did not alter the amount of probe bound. In contrast, ionomycin treatment had strong effects on the intensity of both probes (see also previous report of the effect of ionomycin on MC540, [1]). Thus, it appeared that an important distinction between temperature and ionomycin treatment was that the latter somehow caused the membrane to have higher affinity for these membrane probes.

The results of Fig. 4 suggest that ionomycin treatment destabilizes the membrane in a way that reduces interactions among neighboring lipids thus increasing their spacing and allowing for increased likelihood of probe molecules intercalating among them. Moreover, this destabilization was different from the enhanced fluidity and decreased lipid order associated with a rise in temperature. This idea corroborates prior interpretations that MC540 can be used as an assay of the spacing among membrane lipids [10,29–31]. A reduction in the strength of interactions among neighboring phospholipids has been invoked previously as an explanation for the increase in $sPLA_2$ activity associated with certain structural heterogeneities in artificial membranes and human erythrocytes [3,32–34]. The idea is that such membrane instabilities would allow greater membrane deformability and an increased probability that membrane lipids could protrude sufficiently above the average bilayer surface to enter the active site of bound $sPLA_2$ and be hydrolyzed [6,13,14]. Thus, we conclude that these comparisons between ionomycin treatment and temperature elevation reveal that increased membrane fluidity and lipid disorder are not sufficient to induce susceptibility to $sPLA_2$ unless accompanied by greater average spacing between neighboring lipids.

3.4. Comparison of temperature and ionomycin effects on actin cytoskeleton

The remaining question is: what effect of elevated intracellular calcium would cause such changes to occur in the bilayer? Extracellular exposure of PS might have provided an explanation for greater lipid spacing because of charge exclusion effects from the anionic lipid, but this was rejected based on the data with exogenous PS described above. An obvious alternative is that the instability reflects a loss of interactions between the plasma membrane and the cytoskeleton. This hypothesis is plausible because actin and actin-associated proteins are known to be cleaved/altered during apoptosis [35–38]. Furthermore, ionomycin treatment has recently been shown to disrupt the actin cytoskeleton in S49 cells resulting in destabilization of the bilayer sufficient to accommodate microparticle shedding from the plasma membrane [27]. Biophysically, it is well established that the actin

cytoskeleton stabilizes the membrane (reviewed in [39]) increasing elasticity and thereby creating resistance to deformations such as those associated with cell shape change, microparticle release, and in this case, lipid protrusions that can result in hydrolysis by $sPLA_2$.

If disruption of the actin cytoskeleton is directly relevant to the activity of $sPLA_2$ described in this study, three observations must be true: 1) actin disruption would occur with treatments that also cause the membrane to become susceptible, 2) actin disruption would not occur with an elevation of temperature, and 3) blocking disruption of actin would prevent the ability of ionomycin to induce hydrolysis by $sPLA_2$. Unfortunately, only the first two tests were feasible with S49 cells. Experimental means to directly prevent disruption of the cytoskeleton by ionomycin were not accessible (e.g. calpain inhibitors did not prevent ionomycin-stimulated actin disruption, presumably because of redundant pathways [40]).

To investigate the possibility that ionomycin causes cytoskeletal alterations while temperature does not, F-actin was stained with fluorescent phalloidin and imaged via confocal microscopy. Fig. 5 shows example images of control cells (Panel A), ionomycin-treated cells (Panel B), and cells incubated at 45 °C without ionomycin (Panel C). Fibrous actin filaments were prominent in control cells, and Panel B shows a loss of these filaments and the appearance of large circular aggregates of densely-staining material after ionomycin treatment. Cells incubated at 45 °C for 10 min (Fig. 5C) appeared more like control than ionomycin-treated cells.

ImageJ software was used to calculate the circularity index of all particles in such images as explained in Materials and methods. As shown by the histogram in Fig. 6A, ionomycin treatment reproducibly produced elevated numbers of particles with high circularity (>0.85, Fig. 6B). Previous work has demonstrated that ionomycin stimulates shedding of plasma membrane microparticles to the extracellular fluid [27]. To test the possibility that these highly circular densely-staining particles represented structures associated with the process of particle formation or release, the experiments of Fig. 5 were repeated in the presence of quinine, which is known to prevent microparticle shedding [11,25,27,41] without affecting plasma membrane susceptibility to $sPLA_2$ (Ref. [11] and verified by control experiments on S49 cells, not shown). Fig. 6A demonstrates that the highly- circular particles released with ionomycin treatment were eliminated when quinine was also present (dotted line). Hence, their contribution to quantitative analysis of the images could mostly be excluded by ignoring particles with circularity >0.85. Fig. 6B displays histograms of the size of particles with circularity <0.85. Based on this analysis, the effect of ionomycin on actin filaments separate from changes blockable with quinine was detected by an elevation in the number of particles in the size range of 22 to 44 pixels. At the image magnification used for the analysis, these particles would correspond to a size of ~0.9 to ~1.8 μm^2. As shown in Fig. 6C, both the number of particles in this range and the effect of ionomycin did not vary with temperature (effect of ionomycin = 33% of the variation with $p = 0.0003$, effect of temperature = 8% of the variation with $p = 0.16$, and no significant interaction between the two: $p = 0.98$, n = 2–10 per group). It should be noted that the data in Fig. 6B indicated that only about 44% of the difference between the gray and black bars in Fig. 6C would be completely free from the effect of microparticle release. Nevertheless, the overall effect of ionomycin was still significant even when the effect size was accordingly reduced ($p = 0.0003$ by paired t-test comparing ionomycin samples to their own control samples pooled for all three temperatures, n = 13). This increase in small particles coupled with the loss of stained fibers in the images after ionomycin treatment (Fig. 5B) confirmed previous reports that elevated intracellular calcium produces fragmentation of actin filaments [27,42,43]. Importantly, the absence of such effects with temperature variation supported the idea that these cytoskeletal alterations may be responsible for plasma membrane changes that facilitate hydrolysis by $sPLA_2$.

To further investigate the connection between actin-severing and plasma membrane susceptibility to $sPLA_2$, changes in the actin cytoskeleton were investigated during TG-induced apoptosis. Previous studies have indicated that S49 cells begin to become susceptible to hydrolysis within an hour of exposure to TG, reaching a maximum at 3 h [6]. As shown in Fig. 7, treatment with TG for at least 1 h also caused an increase in the number of low-circularity particles (<0.85) falling within the 0.9–1.8 μm^2 range ($p = 0.004$, paired t-test, n = 5). The magnitude of this increase in small particles was about half that observed in ionomycin-treated samples (Fig. 6), presumably because ionomycin affects the entire population in a more synchronized manner than does TG [1,6].

4. Conclusion

Prior to this study, the understanding of the action of $sPLA_2$ on eukaryotic cells was that membrane order is critical and apparently sufficient to induce rapid hydrolysis [1,2,6,18]. An exception is the human group IIA isoform, which appears to be governed almost entirely by membrane oxidation in S49 cells [44]. Moreover externalization of PS appears to function as a significant enhancer but is insufficient to function alone as the regulator of hydrolysis [2,18]. This study refines those statements with the following four conclusions. First, a simple increase in the motion of the lipids precipitated directly by raising the temperature does not render the membrane susceptible to $sPLA_2$ even though steady state fluorescence data suggest that it produces the same effect on membrane properties as perturbations (such as ionomycin) that do promote hydrolysis (Figs. 1 and 2). Second, although elevation of temperature differed from ionomycin by not causing exposure of PS, that difference is not the determinant of hydrolysis since a combination of elevated temperature plus exposed PS did not induce susceptibility to

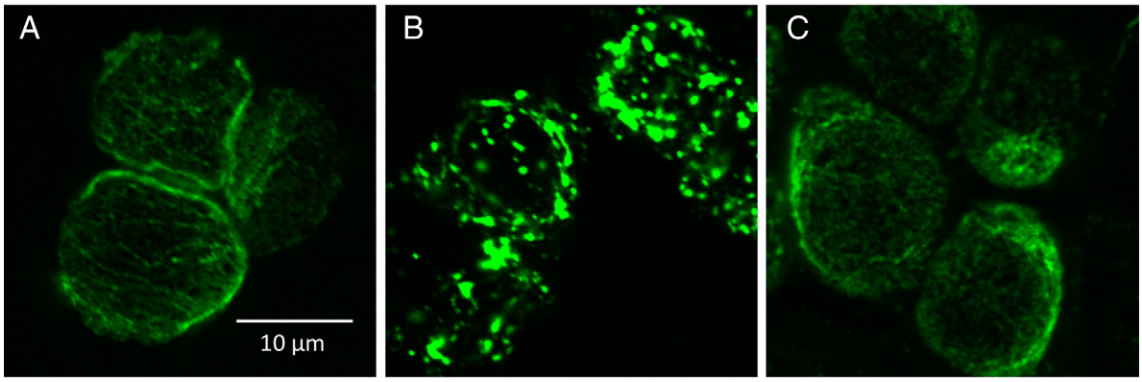

Fig. 5. Images of phalloidin staining of F-actin in control cells (Panel A), ionomycin-treated cells (Panel B), and cells incubated at 45 °C (Panel C). Cells were harvested and equilibrated at the indicated temperature prior to treating for 5 min without (DMSO) or with ionomycin before being mounted onto slides, stained with fluorescent phalloidin, and imaged by confocal microscopy (see Materials and methods). These images were collected with a 60× objective with a 3× digital zoom.

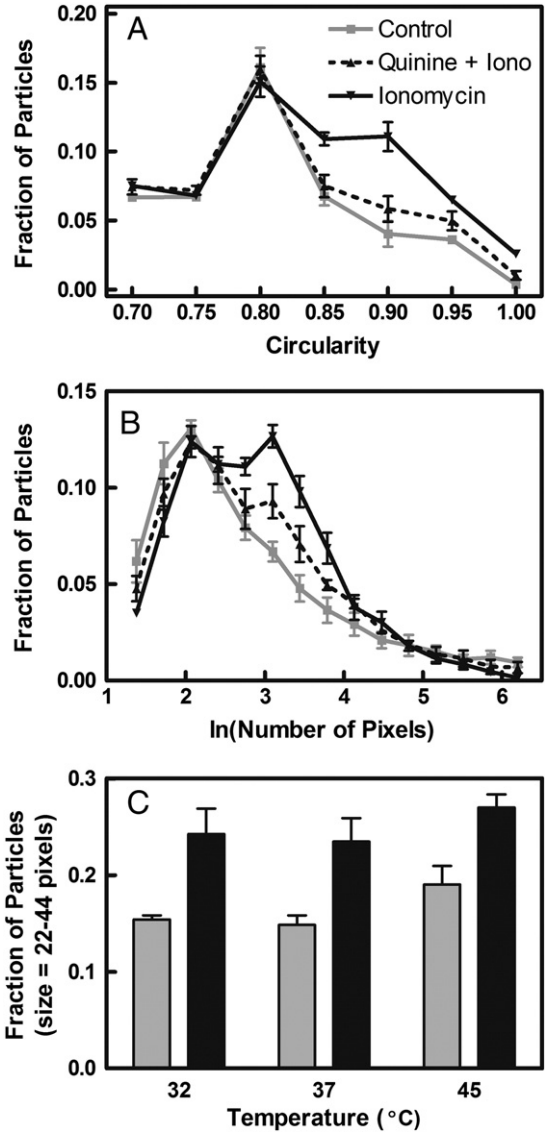

Fig. 6. Effect of temperature and ionomycin on F-actin particle size. Images such as those in Fig. 5 were analyzed using ImageJ as described in Materials and methods. Gray lines and bars represent control samples, solid black lines and bars represent samples treated with ionomycin, and dotted black lines represent samples treated with 1 mM quinine for 10 min prior to addition of ionomycin. Panel A: Histogram of particle circularity (≥0.7, n = 3). Panel B: Histogram of the logarithm of particle size for particles with circularity <0.85 (n = 3). Panel C: The number of particles with circularity <0.85 and in the size range between 22 and 44 pixels was calculated for samples at the indicated temperatures (n = 2–10) and normalized to the total number of particles with circularity <0.85.

sPLA$_2$. Third, measurements of Patman, MC540, and TMA-DPH fluorescence intensities identified a distinction between the effect of temperature and ionomycin. In the former case, the membrane environment detected by the probe became more polar as temperature increased. In the latter, treatments that promote hydrolysis also enhanced the insertion of probes into the membrane (Fig. 4). This effect on probe partitioning has been hypothesized to reflect a reduction in membrane lipid-neighbor interactions which could raise the probability of vertical lipid fluctuations in the membrane sufficient to facilitate binding of substrate to the enzyme active site [6,13,14]. Fourth, based on the data of Figs. 5–7, it is suggested that the biochemical basis for the altered probe distribution is due to disruption of the actin cytoskeleton. Since it was not possible to block the effect of ionomycin to disrupt the cytoskeleton, this fourth conclusion must remain a proposal for further testing in the future.

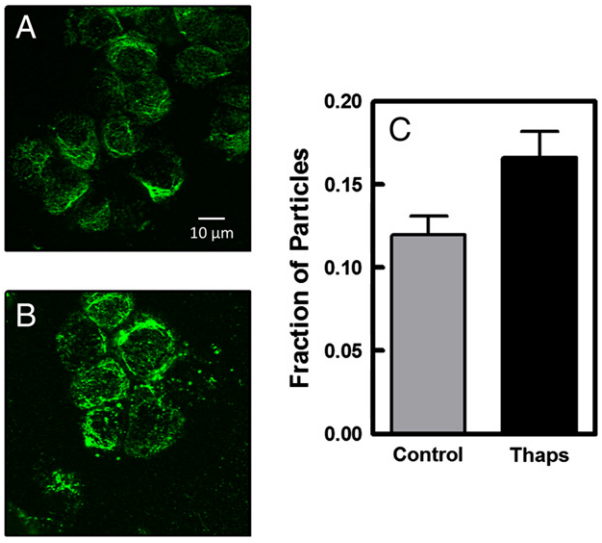

Fig. 7. Actin fragmentation during TG-induced apoptosis. Panels A and B are confocal images of phalloidin-stained F-actin after 4 h of treatment with DMSO (vehicle control, Panel A) or TG (Panel B). Samples were prepared as in Fig. 5 without the digital zoom. Panel C: Images were analyzed as in Fig. 6, and the fraction of particles with circularity <0.85 in the size range of 22–44 pixels was calculated. The gray bar represents control samples (n = 5), and the black bar represents samples treated for 1–5 h with TG (n = 5; each experimental sample represents the average from multiple images at multiple time points within the 1–5 h; linear regression revealed no time trend in that range, $p = 0.9$, $r^2 = 0.0007$).

References

[1] R.W. Bailey, E.D. Olson, M.P. Vu, T.J. Brueseke, L. Robertson, R.E. Christensen, K.H. Parker, A.M. Judd, J.D. Bell, Relationship between membrane physical properties and secretory phospholipase A2 hydrolysis kinetics in S49 cells during ionophore-induced apoptosis, Biophys. J. 93 (2007) 2350–2362.
[2] R.W. Bailey, T. Nguyen, L. Robertson, E. Gibbons, J. Nelson, R.E. Christensen, J.P. Bell, A.M. Judd, J.D. Bell, Sequence of physical changes to the cell membrane during glucocorticoid-induced apoptosis in S49 lymphoma cells, Biophys. J. 96 (2009) 2709–2718.
[3] K.B. Best, A.J. Ohran, A.C. Hawes, T.L. Hazlett, E. Gratton, A.M. Judd, J.D. Bell, Relationship between erythrocyte membrane phase properties and susceptibility to secretory phospholipase A2, Biochemistry 41 (2002) 13982–13988.
[4] F.M. Harris, S.K. Smith, J.D. Bell, Physical properties of erythrocyte ghosts that determine susceptibility to secretory phospholipase A2, J. Biol. Chem. 276 (2001) 22722–22731.
[5] A.L. Heiner, E. Gibbons, J.L. Fairbourn, L.J. Gonzalez, C.O. McLemore, T.J. Brueseke, A.M. Judd, J.D. Bell, Effects of cholesterol on physical properties of human erythrocyte membranes: impact on susceptibility to hydrolysis by secretory phospholipase A2, Biophys. J. 94 (2008) 3084–3093.
[6] E. Gibbons, K.R. Pickett, M.C. Streeter, A.O. Warcup, J. Nelson, A.M. Judd, J.D. Bell, Molecular details of membrane fluidity changes during apoptosis and relationship to phospholipase A(2) activity, Biochim. Biophys. Acta 1828 (2013) 887–895.
[7] J. Nelson, L.L. Francom, L. Anderson, K. Damm, R. Baker, J. Chen, S. Franklin, A. Hamaker, I. Izidoro, E. Moss, M. Orton, E. Stevens, C. Yeung, A.M. Judd, J.D. Bell, Investigation into the role of phosphatidylserine in modifying the susceptibility of human lymphocytes to secretory phospholipase A(2) using cells deficient in the expression of scramblase, Biochim. Biophys. Acta 1818 (2012) 1196–1204.
[8] J.D. Bell, M. Burnside, J.A. Owen, M.L. Royall, M.L. Baker, Relationships between bilayer structure and phospholipase A2 activity: interactions among temperature, diacylglycerol, lysolecithin, palmitic acid, and dipalmitoylphosphatidylcholine, Biochemistry 35 (1996) 4945–4955.
[9] H. Franchino, E. Stevens, J. Nelson, T.A. Bell, J.D. Bell, Wavelength dependence of patman equilibration dynamics in phosphatidylcholine bilayers, Biochim. Biophys. Acta 1828 (2013) 877–886.
[10] H.A. Wilson-Ashworth, Q. Bahm, J. Erickson, A. Shinkle, M.P. Vu, D. Woodbury, J.D. Bell, Differential detection of phospholipid fluidity, order, and spacing by fluorescence spectroscopy of bis-pyrene, prodan, nystatin, and merocyanine 540, Biophys. J. 91 (2006) 4091–4101.
[11] S.K. Smith, A.R. Farnbach, F.M. Harris, A.C. Hawes, L.R. Jackson, A.M. Judd, R.S. Vest, S. Sanchez, J.D. Bell, Mechanisms by which intracellular calcium induces susceptibility to secretory phospholipase A2 in human erythrocytes, J. Biol. Chem. 276 (2001) 22732–22741.
[12] J.R. Lakowicz, D.R. Bevan, B.P. Maliwal, H. Cherek, A. Balter, Synthesis and characterization of a fluorescence probe of the phase transition and dynamic properties of membranes, Biochemistry 22 (1983) 5714–5722.
[13] P. Hoyrup, T.H. Callisen, M.O. Jensen, A. Halperin, O.G. Mouritsen, Lipid protrusions, membrane softness, and enzymatic activity, Phys. Chem. Chem. Phys. 6 (2004) 1608–1615.

[14] A. Halperin, O.G. Mouritsen, Role of lipid protrusions in the function of interfacial enzymes, Eur. Biophys. J. 34 (2005) 967–971.
[15] G. Atsumi, M. Murakami, M. Tajima, S. Shimbara, N. Hara, I. Kudo, The perturbed membrane of cells undergoing apoptosis is susceptible to type II secretory phospholipase A2 to liberate arachidonic acid, Biochim. Biophys. Acta 1349 (1997) 43–54.
[16] J.M. Maraganore, G. Merutka, W. Cho, W. Welches, F.J. Kezdy, R.L. Heinrikson, A new class of phospholipases A2 with lysine in place of aspartate 49. Functional consequences for calcium and substrate binding, J. Biol. Chem. 259 (1984) 13839–13843.
[17] H.A. Wilson, W. Huang, J.B. Waldrip, A.M. Judd, L.P. Vernon, J.D. Bell, Mechanisms by which thionin induces susceptibility of S49 cell membranes to extracellular phospholipase A2, Biochim. Biophys. Acta 1349 (1997) 142–156.
[18] E.D. Olson, J. Nelson, K. Griffith, T. Nguyen, M. Streeter, H.A. Wilson-Ashworth, M.H. Gelb, A.M. Judd, J.D. Bell, Kinetic evaluation of cell membrane hydrolysis during apoptosis by human isoforms of secretory phospholipase A2, J. Biol. Chem. 285 (2010) 10993–11002.
[19] G.V. Richieri, A.M. Kleinfeld, Continuous measurement of phospholipase A2 activity using the fluorescent probe ADIFAB, Anal. Biochem. 229 (1995) 256–263.
[20] T. Parasassi, G. De Stasio, G. Ravagnan, R.M. Rusch, E. Gratton, Quantitation of lipid phases in phospholipid vesicles by the generalized polarization of Laurdan fluorescence, Biophys. J. 60 (1991) 179–189.
[21] C.A. Schneider, W.S. Rasband, K.W. Eliceiri, NIH Image to ImageJ: 25 years of image analysis, Nat. Methods 9 (2012) 671–675.
[22] Q. Zhou, J. Zhao, J.G. Stout, R.A. Luhm, T. Wiedmer, P.J. Sims, Molecular cloning of human plasma membrane phospholipid scramblase. A protein mediating transbilayer movement of plasma membrane phospholipids, J. Biol. Chem. 272 (1997) 18240–18244.
[23] E.M. Bevers, P. Comfurius, R.F. Zwaal, Changes in membrane phospholipid distribution during platelet activation, Biochim. Biophys. Acta 736 (1983) 57–66.
[24] K.H. Nielson, C.A. Olsen, D.V. Allred, K.L. O'Neill, G.F. Burton, J.D. Bell, Susceptibility of S49 lymphoma cell membranes to hydrolysis by secretory phospholipase A(2) during early phase of apoptosis, Biochim. Biophys. Acta 1484 (2000) 163–174.
[25] D. Allan, P. Thomas, Ca2 + -induced biochemical changes in human erythrocytes and their relation to microvesiculation, Biochem. J. 198 (1981) 433–440.
[26] H.A. Wilson, J.B. Waldrip, K.H. Nielson, A.M. Judd, S.K. Han, W. Cho, P.J. Sims, J.D. Bell, Mechanisms by which elevated intracellular calcium induces S49 cell membranes to become susceptible to the action of secretory phospholipase A2, J. Biol. Chem. 274 (1999) 11494–11504.
[27] L.E. Campbell, J. Nelson, E. Gibbons, A.M. Judd, J.D. Bell, Membrane properties involved in calcium-stimulated microparticle release from the plasma membranes of S49 lymphoma cells, TheScientificWorldJournal 2014 (2014) (Article ID 537192).
[28] G. Parisio, A. Marini, A. Biancardi, A. Ferrarini, B. Mennucci, Polarity-sensitive fluorescent probes in lipid bilayers: bridging spectroscopic behavior and microenvironment properties, J. Phys. Chem. B 115 (2011) 9980–9989.
[29] H.A. Franchino, B.C. Johnson, S.K. Neeley, R.B. Tajhya, M.P. Vu, H.A. Wilson-Ashworth, J.D. Bell, Combined use of steady-state fluorescence emission and anisotropy of merocyanine 540 to distinguish crystalline, gel, ripple, and liquid crystalline phases in dipalmitoylphosphatidylcholine bilayers, PMC Biophys. 3 (2010) 14.
[30] W. Stillwell, S.R. Wassall, A.C. Dumaual, W.D. Ehringer, C.W. Browning, L.J. Jenski, Use of merocyanine (MC540) in quantifying lipid domains and packing in phospholipid vesicles and tumor cells, Biochim. Biophys. Acta 1146 (1993) 136–144.
[31] B.M. Stott, M.P. Vu, C.O. McLemore, M.S. Lund, E. Gibbons, T.J. Brueseke, H.A. Wilson-Ashworth, J.D. Bell, Use of fluorescence to determine the effects of cholesterol on lipid behavior in sphingomyelin liposomes and erythrocyte membranes, J. Lipid Res. 49 (2008) 1202–1215.
[32] J.B. Henshaw, C.A. Olsen, A.R. Farnbach, K.H. Nielson, J.D. Bell, Definition of the specific roles of lysolecithin and palmitic acid in altering the susceptibility of dipalmitoylphosphatidylcholine bilayers to phospholipase A2, Biochemistry 37 (1998) 10709–10721.
[33] W.R. Burack, A.R. Dibble, M.M. Allietta, R.L. Biltonen, Changes in vesicle morphology induced by lateral phase separation modulate phospholipase A2 activity, Biochemistry 36 (1997) 10551–10557.
[34] C. Leidy, L. Linderoth, T.L. Andresen, O.G. Mouritsen, K. Jorgensen, G.H. Peters, Domain-induced activation of human phospholipase A2 type IIA: local versus global lipid composition, Biophys. J. 90 (2006) 3165–3175.
[35] K.K. Wang, Calpain and caspase: can you tell the difference? Trends Neurosci. 23 (2000) 20–26.
[36] V.E. Franklin-Tong, C.W. Gourlay, A role for actin in regulating apoptosis/programmed cell death: evidence spanning yeast, plants and animals, Biochem. J. 413 (2008) 389–404.
[37] C.W. Gourlay, K.R. Ayscough, The actin cytoskeleton: a key regulator of apoptosis and ageing? Nat. Rev. Mol. Cell Biol. 6 (2005) 583–589.
[38] J.E. Leadsham, V.N. Kotiadis, D.J. Tarrant, C.W. Gourlay, Apoptosis and the yeast actin cytoskeleton, Cell Death Differ. 17 (2010) 754–762.
[39] J. Gilden, M.F. Krummel, Control of cortical rigidity by the cytoskeleton: emerging roles for septins, Cytoskeleton 67 (2010) 477–486.
[40] S. Montoro-Garcia, E. Shantsila, F. Marin, A. Blann, G.Y. Lip, Circulating microparticles: new insights into the biochemical basis of microparticle release and activity, Basic Res. Cardiol. 106 (2011) 911–923.
[41] E. Reichstein, A. Rothstein, Effects of quinine on Ca++-induced K + efflux from human red blood cells, J. Membr. Biol. 59 (1981) 57–63.
[42] F. Basse, P. Gaffet, A. Bienvenue, Correlation between inhibition of cytoskeleton proteolysis and anti-vesiculation effect of calpeptin during A23187-induced activation of human platelets: are vesicles shed by filopod fragmentation? Biochim. Biophys. Acta 1190 (1994) 217–224.
[43] D.J. Kwiatkowski, Functions of gelsolin: motility, signaling, apoptosis, cancer, Curr. Opin. Cell Biol. 11 (1999) 103–108.
[44] E. Gibbons, J. Nelson, L. Anderson, K. Brewer, S. Melchor, A.M. Judd, J.D. Bell, Role of membrane oxidation in controlling the activity of human group IIa secretory phospholipase A(2) toward apoptotic lymphoma cells, Biochim. Biophys. Acta 1828 (2013) 670–676.